Online Appendix for "Local Projections or VARs? A Primer for Macroeconomists"

José Luis Montiel Olea Mikkel Plagborg-Møller
Eric Qian Christian K. Wolf

May 22, 2025

This online appendix contains supplemental material on: the comparison of LP and VAR estimation results in prior empirical work (Supplemental Appendix A); implementation details for the LP and VAR estimators that we consider in our simulations (Supplemental Appendix B); a detailed description of our simulation study set-up (Supplemental Appendix C); further simulation results (Supplemental Appendix D); theoretical and simulation-based discussion of the probability of the event that the VAR point estimate falls outside of the LP confidence interval (Supplemental Appendix E).

Appendix A VARs vs. LPs in empirical work

We describe how we construct the point estimate and standard error comparison of LPs and VARs in existing applied work in Figure 3.1. Our implementation closely follows our earlier work in Montiel Olea, Plagborg-Møller, Qian, and Wolf (2024, Online Appendix C), which in turn is based on the literature summary in Ramey (2016).

We consider four applications in which the researcher has access to a direct measure of a structural shock: to monetary policy, taxes, government spending, and technology. She then estimates the dynamic causal effects of these macroeconomic shocks using either LP or the equivalent (internal-instrument) recursive VAR. The choice of shocks, outcomes, controls, and lags is exactly the same as in our earlier work, as is the computation of standard errors. Overall we obtain LP and VAR impulse response point estimates and standard errors for 385 impulse responses, across all shocks, outcome variables, and horizons. For each we compute

standard error ratios and point estimate differences, scaled by the VAR standard error. We finally split the impulse responses into short horizons ($\leq$ one year, 84 observations overall) and long horizons ($>$ one year, 301 observations overall), and report our results for standard error ratios and scaled point estimate differences as boxplots.

Appendix B Estimation method details

We provide implementation details for the LP and VAR estimator variants that we consider in our simulations in Sections 5.2 and 6.4.

B.1 LPs

Recall from Section 2 that the LP estimator of the horizon-h impulse response is the coefficient $\hat{\beta}_h$ in the h-step-ahead regression

$$y_{t+h} = \hat{\mu}_h + \hat{\theta}_h^{\text{LP}} x_t + \hat{\gamma}_h' r_t + \sum_{\ell=1}^{p} \hat{\delta}_{h,\ell}' w_{t-\ell} + \hat{\xi}_{h,t}. \tag{B.1}$$

For our different structural identification schemes, the outcome, impulse, and control variables are selected as follows:

1. *Observed shock.* x_t is the observed shock $\varepsilon_{1,t}$, there are no contemporaneous controls r_t, and the outcome variable y_t is selected at random from the observed data series. The lagged controls are either the shock plus the full five-dimensional vector of observables, or only the shock plus the outcome of interest.

2. *Recursive identification.* x_t is the policy variable (i.e., either the federal funds rate or government purchases), r_t contains all the variables ordered before x_t in the structural shock identification scheme, and w_t always contains the full vector of observables, consistent with the invertibility assumption.

We consider the bias-corrected version of the LP estimator. We follow Herbst and Johannsen (2024) for the bias correction, using their approximate analytical bias formula for LPs with controls.[B.1] The lag length p is either set exogenously (in our simulations typically

[B.1] We substitute population autocovariances with sample analogues. We implement an iterative bias correction described in Equation 11 of Herbst and Johannsen (2024), with the impulse response estimate at horizon h bias-corrected using the previously corrected impulse response estimates at horizons $1, 2, \ldots, h-1$.

to $p = 4$) or selected using the Akaike Information Criterion (AIC) applied to a reduced-form VAR in the observed variables. We use Eicker-Huber-White standard errors, and a modification of the bootstrap routine for lag-augmented local projections suggested in Montiel Olea and Plagborg-Møller (2021). An important difference is that instead of using the wild autoregressive bootstrap design, we use the autoregressive residual block bootstrap of Brüggemann, Jentsch, and Trenkler (2016). As implied by the results of Brüggemann, Jentsch, and Trenkler (2016), this is important in order to conduct inference on *structural* impulse responses (rather than reduced-form impulse responses). A description of the algorithm is as follows:

1. Compute the LP-based structural impulse response estimate of interest and its standard error.

2. Estimate the VAR(p) model by OLS. Compute the corresponding VAR residuals $\hat{u}_t$. Bias-adjust the VAR coefficients using the formula in Pope (1990).

3. Compute the structural impulse response of interest implied by the VAR model.

4. For each bootstrap iteration $b = 1, \dots, B$:

   i) Generate properly centered bootstrap residuals $\hat{u}_t^*$ using steps 2 and 3 of the residual-based moving block bootstrap scheme in Brüggemann, Jentsch, and Trenkler (2016), as described on p. 73 of their paper (see their Section 4). The block size is chosen using the rule described on p. 2665 of Jentsch and Lunsford (2019).[B.2]

   ii) Draw a block of p initial observations $(y_1^*, \dots, y_p^*)$ uniformly at random from the $T - p + 1$ blocks of p observations in the original data.

   iii) Generate bootstrap data y_t^*, $t = p + 1, \dots, T$, by iterating on the bias-corrected VAR(p) model estimated in step 2, using the innovations $\hat{u}_t^*$.

   iv) Apply the LP estimator to the bootstrap data $\{y_t^*\}$ and compute its Eicker-Huber-White standard error.

   v) Store the t-statistic for the LP estimate, making sure that the statistic is centered around the VAR-implied structural impulse response from step 3. As explained by Montiel Olea and Plagborg-Møller (2021), it is critical that the bootstrap t-statistic is centered at the VAR-implied impulse response (see step 4(v) on p. 1808 of that paper), not the LP estimate from step 1.

[B.2] The rule gives a block size of 20 for our sample size of $T = 240$.

5. Compute the $a/2$ and $1-a/2$ quantiles of the B draws of the t-statistic, $b = 1, \ldots, B$.

6. Return the percentile-t bootstrap confidence interval (e.g., Montiel Olea and Plagborg-Møller, 2021, step 6, p. 1808).

We also consider a shrinkage variant of LP, the penalized LP of Barnichon and Brownlees (2019). As suggested by those authors, we model impulse responses using B-spline basis functions, and penalize deviations from a quadratic function of the impulse response horizon h, up to 20, with the penalty parameter selected using 5-fold cross-validation. For confidence intervals we similarly follow the suggestions of the authors, using their heuristic procedure (see p. 525), with the exact same undersmoothing to reduce the bias induced by shrinkage.

B.2 VARs

Recall from Section 2 that the VAR impulse response estimator is based on the reduced-form VAR

$$w_t = \hat{c} + \sum_{\ell=1}^{p} \hat{A}_\ell w_{t-\ell} + \hat{u}_t. \tag{B.2}$$

with $\text{Var}(u_t) = \hat{B}\hat{B}'$ where $\hat{B}$ is the Cholesky decomposition of the estimated forecast error variance-covariance matrix. The two identification schemes are implemented as follows:

1. **Observed shock.** w_t contains the observed shock as well as either all other five observed series, or only the outcome variable of interest. The observed shock is ordered first in the recursive orthogonalization of the reduced-form innovations.

2. **Recursive identification.** w_t consists of the five observed series, ordered as indicated in our discussion of the structural monetary and fiscal shock identification schemes (see Supplemental Appendix C.2). We do not consider a small version of this system, consistent with the invertibility assumption.

The reduced-form VAR coefficient matrices are estimated using the analytical bias correction of Pope (1990), following the recommendations in Kilian (1998). The lag length p is either set exogenously (in our simulations typically to $p = 4$) or selected using the AIC for (B.2). We use Eicker-Huber-White standard errors, and bootstrap VAR estimates using the residual block bootstrap of Brüggemann, Jentsch, and Trenkler (2016). The block size is chosen using the rule of thumb of Jentsch and Lunsford (2019, p. 2665), giving a block

size of 20 for our sample size of $T = 240$. Following the recommendation of Inoue and Kilian (2020), we report the Efron bootstrap confidence interval.

For shrinkage, we estimate a Bayesian VAR using the default prior recommendations of Giannone, Lenza, and Primiceri (2015), largely following their replication code, though with some minor adjustments as discussed in Li, Plagborg-Møller, and Wolf (2024, Appendix B). We draw 500 times from the posterior, reporting posterior means of the impulse responses (for our bias-variance trade-off plots) and constructing posterior credible intervals using 5th and 95th percentiles (for uncertainty assessments).

Appendix C Simulation study details

C.1 DFM estimation

We estimate the encompassing stationary and non-stationary DFMs on the data set of Stock and Watson (2016), proceeding as in Li, Plagborg-Møller, and Wolf (2024), but additionally allowing for ARCH disturbances. For the stationary DFM, we follow the exact same steps as in Online Appendix F.2 (p. 16) of Li, Plagborg-Møller, and Wolf, which in turn replicates the original analysis by Stock and Watson as well as in Lazarus, Lewis, Stock, and Watson (2018). For the non-stationary DFM, we first transform variables, then select the number of factors and lags, and finally estimate the factor VECM just as in Online Appendix C (pp. 2–4) of Li, Plagborg-Møller, and Wolf.

To better capture likely challenges for inference in applied practice, we generalize the estimated DFMs by allowing for heteroskedastic errors. Specifically, given the DFM estimated in the first step, we next estimate separate ARCH(1) models for the *reduced-form* residuals in the factor and idiosyncratic equations. For the simulation DGP, we conservatively model the *structural* shocks to the factors as following independent ARCH(1) models with ARCH coefficient equal to the maximum of the estimated reduced-form factor ARCH coefficients; for the idiosyncratic innovations we just directly use the estimated actual ARCH coefficients, censored above at 0.7 (this censoring affects only a handful of series and is consistent with the estimated confidence intervals).

C.2 DGP selection and impulse response estimands

We draw our individual DGPs from the two encompassing DFMs by proceeding as follows. For all DGPs, we restrict attention to the following 17 oft-used series (with Stock and Watson

Data Appendix series # in brackets): *real GDP (1); real consumption (2); real investment (6); real government expenditure (12); the unemployment rate (56); personal consumption expenditure prices (95); the GDP deflator (97); the core consumer price index (121); average hourly earnings (132); the federal funds rate (142); the 10-year Treasury rate (147); the BAA 10-year spread (151); an index of the U.S. dollar exchange rate relative to other major currencies (172); the S&P 500 (181); a real house price index (193); consumer expectations (196); and real oil prices (202).* We then draw several random combinations of five series from this overall set of salient time series, subject to the constraint that each DGP contains either the federal funds rate or government spending (for monetary or fiscal shock estimands, respectively, as discussed further below) as well as at least one real activity series (categories 1–3 in the Stock and Watson data appendix) and one price series (category 6). For both the stationary and non-stationary DFM we draw 100 monetary and 100 fiscal DGPs in this way.

Observed shock identification. We define the monetary policy shock as the (unique) linear combination of the innovations in the factor equation that maximizes the impact impulse response of the federal funds rate, and analogously for the fiscal policy shock, with government spending as the maximized response variable. We then assume that the econometrician directly observes this shock of interest, together with the five observables drawn from the list of salient time series, as we discussed above. She estimates the propagation of the shock using either LPs with the shock as the impulse variable (and no contemporaneous controls) or a recursive VAR with the observed shock ordered first. The outcome of interest is randomly selected among the observable series, not including the fiscal or monetary policy instruments (i.e., government purchases or the federal funds rate).

We also estimate LP and VAR specifications that use a smaller set of observables. Here the system only contains the observed shock as well as the outcome variable of interest.

Recursive identification. For recursive identification, the researcher only observes the five time series drawn from the encompassing DFM. We then define as the object of interest impulse responses with respect to a recursive orthogonalization of the reduced-form (Wold) forecast errors in the VAR(∞) representation of the observables. For monetary policy, we order the federal funds rate last and then call the orthogonalized innovation to that variable a monetary policy shock, restricting all other variables to not respond contemporaneously to monetary policy, as in Christiano, Eichenbaum, and Evans (1999). For fiscal policy, we order government spending first and then call the innovation to that variable a fiscal policy shock, thus restricting the fiscal authority to respond to all of the other innovations with

a lag, following Blanchard and Perotti (2002). See Li, Plagborg-Møller, and Wolf (2024, Online Appendix D) for further details.

C.3 Population estimands

For our visual illustration of LP-VAR equivalence in Figure 2.1 we consider one particular monetary policy DGP from the stationary DFM, with recursive shock identification. The observables in our system are (Stock and Watson Data Appendix series # in brackets): the unemployment rate (56); real GDP (1); the core consumer price index (121); the BAA 10-year spread (151); and the federal funds rate (142). The outcome of interest is unemployment. We then simulate a large sample, and use recursive LPs and VARs with $p \in \{2, 6, 12\}$ lags to estimate the propagation of the recursively identified monetary shock, as discussed above. We compare these finite-lag LP and VAR estimands with the true population projection on the recursively identified monetary policy innovation, which we estimate using a numerical approximation to an infinite-lag VAR.

C.4 Degree of misspecification

Given a DGP—i.e., a five-variable (for recursive identification) or six-variable (for observed shock identification) system randomly drawn from the encompassing DFM—and a lag length p, we can represent that DGP as a VARMA(p,∞), following the same steps as those outlined in Montiel Olea, Plagborg-Møller, Qian, and Wolf (2024, Footnote 8). We then obtain the total degree of misspecification as

$$\sqrt{T \times \mathcal{M}} = \|\alpha(L)\| \equiv \sqrt{\sum_{\ell=1}^{\infty} \text{trace}\{D\alpha_\ell' D^{-1} \alpha_\ell\}},$$

where D is the variance-covariance matrix of the contemporaneous innovations. Please note that this computation is relevant only for Footnote 18, where we report the average degree of misspecification across our stationary DGPs.

Appendix D Supplementary simulation results

We provide several supplementary simulation results to complement our main findings reported in Sections 5.2 and 6.4. We here report detailed results for: recursive identification;

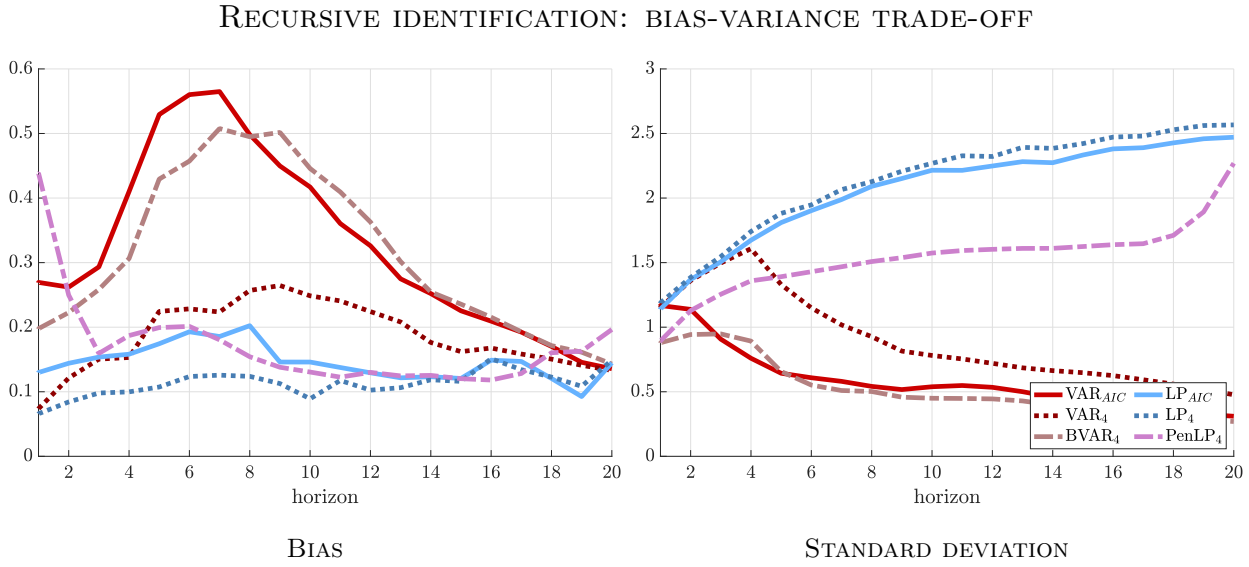

Figure D.1: Median (across DGPs) of absolute bias $\left|\mathbb{E}\left[\hat{\theta}_h - \theta_h\right]\right|$ (left panel) and standard deviation $\sqrt{\text{Var}(\hat{\theta}_h)}$ (right panel) of the different estimation procedures, relative to $\sqrt{\frac{1}{21}\sum_{h=0}^{20}\theta_h^2}$.

monetary and fiscal policy shocks considered separately; as well as average confidence interval coverage and width.

D.1 Recursive identification

While our headline results in Sections 5.2 and 6.4 are reported for observed shock identification, broadly similar lessons for both the bias-variance trade-off and for inference emerge under recursive shock identification. Visual summaries are provided in Figures D.1 and D.2.

Figure D.1 shows the bias-variance trade-off, now in the interest of space averaging across both monetary and fiscal shocks and across stationary and non-stationary DGPs. We see the same patterns as for observed shock identification: the bias-variance trade-off is stark, long lag lengths for the VAR align it with LPs, and the variance cost of LPs is large. Differently from the observed shock case, we do not report any results for "small" specifications, simply because the control vector is now integral to the economic identifying assumptions.

Figure D.2 displays the coverage of confidence intervals, again across all DGPs. As in the observed shock case, VARs with lag length selected by standard information criteria significantly undercover, while LPs tend to cover well, in particular with bootstrapped confidence intervals. Also as for observed shocks, bootstrapping is particularly important for accurate long-horizon coverage in the non-stationary DGPs. Finally we now also see that inclusion of

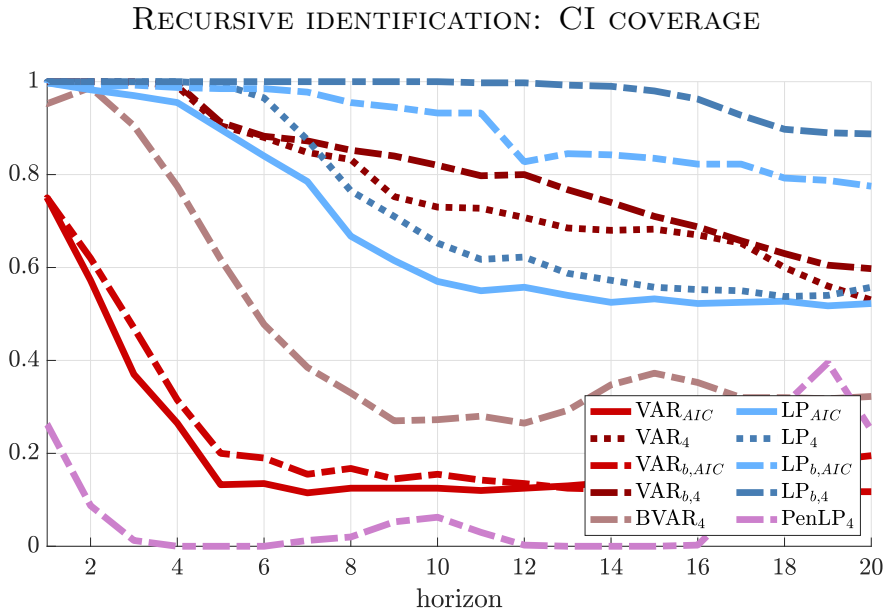

Figure D.2: Fraction of DGPs (both stationary and non-stationary) for which the confidence interval coverage probability exceeds 80%. See caption for Figure 6.2 for an explanation of the abbreviations in the legend.

longer lag lengths is more important for LP, simply because those lags now matter for the structural identification scheme, ensuring that the shock of interest is indeed spanned by the regression residuals.

D.2 Fiscal and monetary shocks

Our reported conclusions are not sensitive to the type of (policy) shock that we consider. To establish this, Figures D.3 and D.4 show bias, variance, and coverage results for fiscal shocks (combining stationary and non-stationary DGPs), while Figures D.3 and D.4 do the same for monetary shocks. The figures by shock echo the messages of our main figures, which average across shocks: there is a meaningful bias-variance trade-off; the variance cost of LPs is high; and only LP methods robustly attain high coverage.

D.3 Coverage probability and CI width

While in Section 6.4 we report the fraction of LP and VAR confidence intervals with coverage above 80%, Figure D.7 here instead shows the coverage probability (left panel) and median confidence interval length (right panel) of our different inference procedures *averaged* across all DGPs, both stationary and non-stationary. Before averaging the coverage probabilities

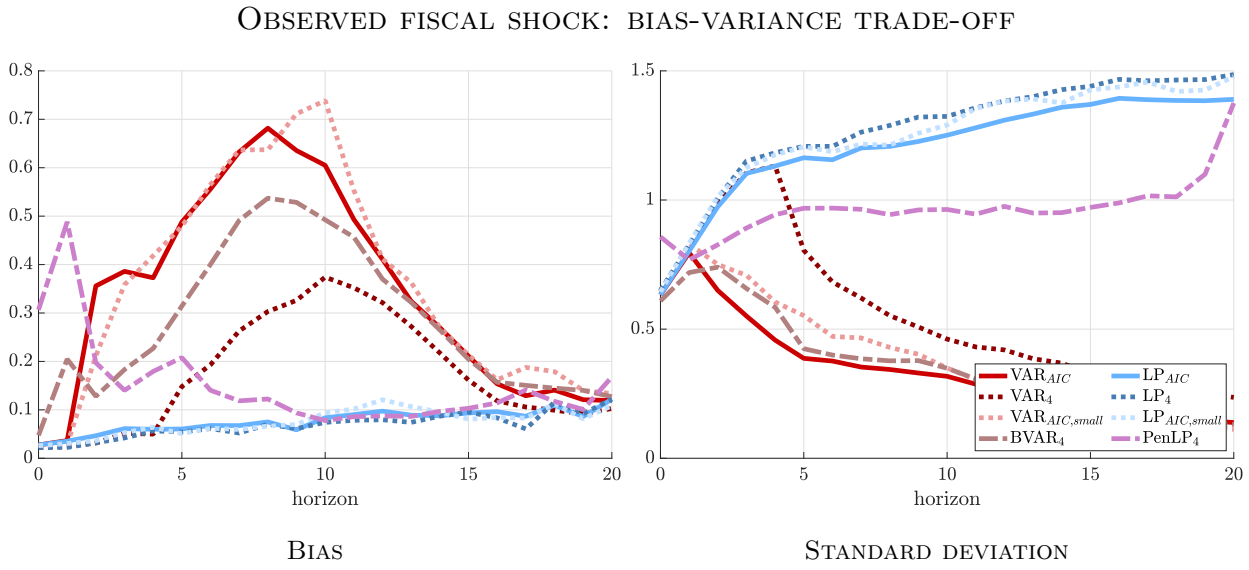

Figure D.3: Median (across DGPs) of absolute bias $\left|\mathbb{E}\left[\hat{\theta}_h - \theta_h\right]\right|$ (left panel) and standard deviation $\sqrt{\text{Var}(\hat{\theta}_h)}$ (right panel) of the different estimation procedures, relative to $\sqrt{\frac{1}{21}\sum_{h=0}^{20}\theta_h^2}$.

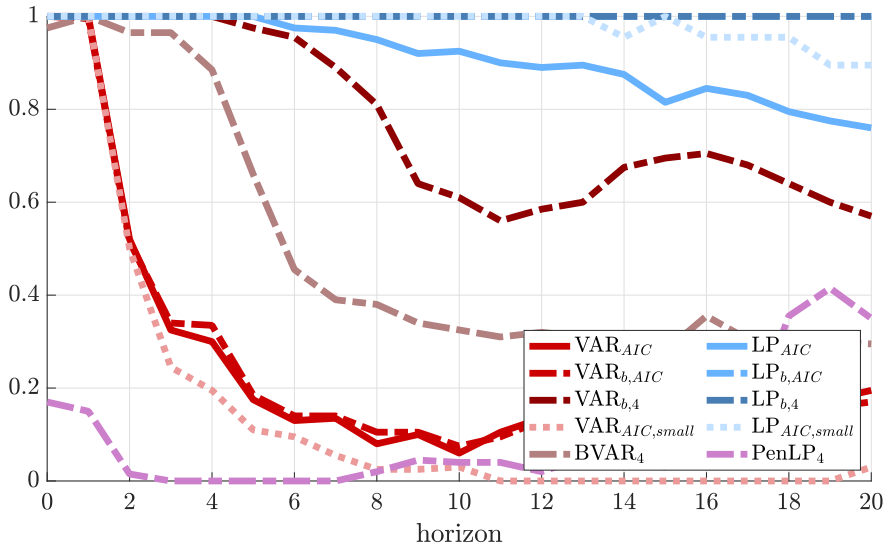

Figure D.4: Fraction of DGPs (both stationary and non-stationary) for which the confidence interval coverage probability exceeds 80%. See caption for Figure 6.2 for an explanation of the abbreviations in the legend.

Observed monetary shock: bias-variance trade-off

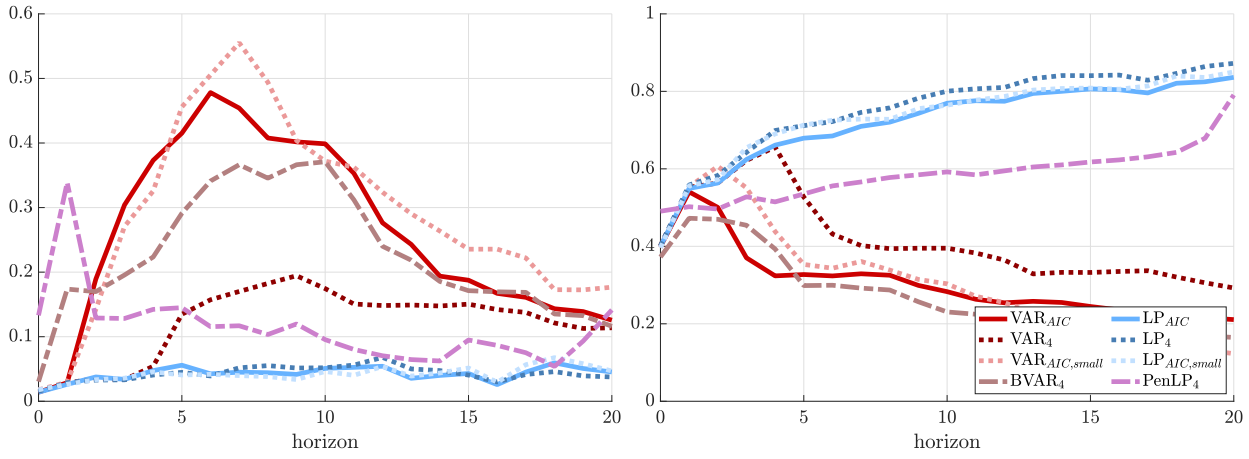

Bias Standard deviation

Figure D.5: Median (across DGPs) of absolute bias $\left|\mathbb{E}\left[\hat{\theta}_h - \theta_h\right]\right|$ (left panel) and standard deviation $\sqrt{\text{Var}(\hat{\theta}_h)}$ (right panel) of the different estimation procedures, relative to $\sqrt{\frac{1}{21}\sum_{h=0}^{20}\theta_h^2}$.

Observed monetary shock: CI coverage

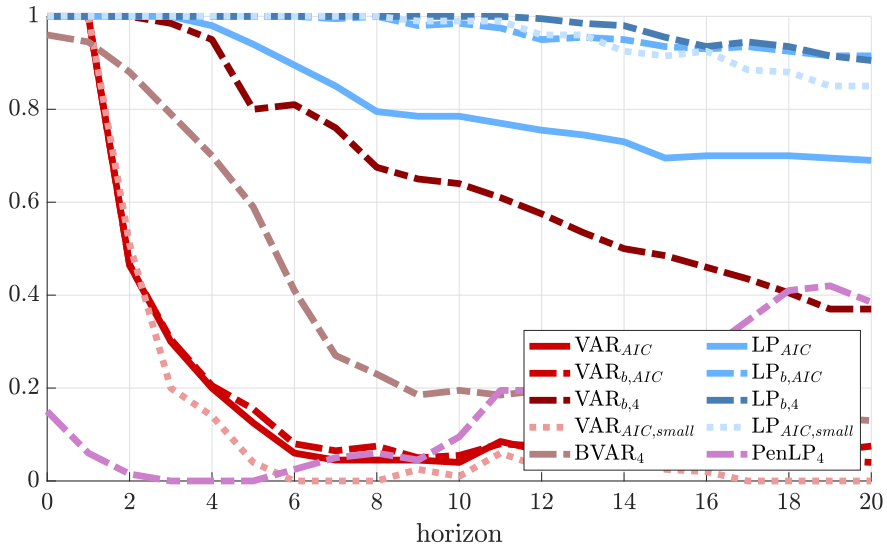

Figure D.6: Fraction of DGPs (both stationary and non-stationary) for which the confidence interval coverage probability exceeds 80%. See caption for Figure 6.2 for an explanation of the abbreviations in the legend.

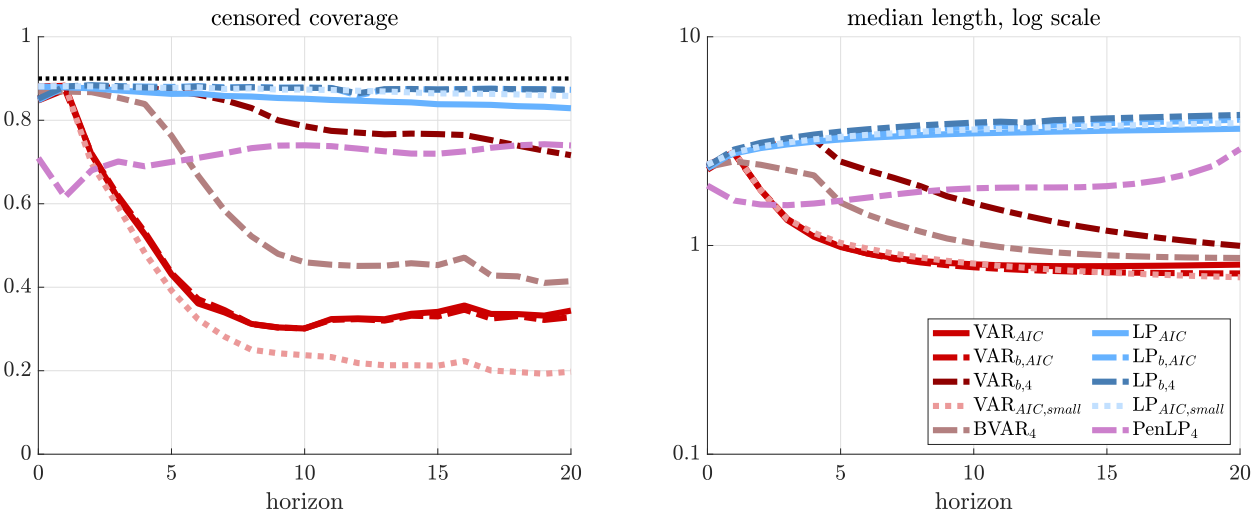

Figure D.7: Coverage probabilities (left panel, coverage is censored above at 90%) and median confidence interval length (right panel) for VAR (red) and LP (blue) confidence intervals, averaged across all DGPs (both stationary and non-stationary) separately at each horizon. The right panel normalizes the interval length by the overall magnitude $\sqrt{\frac{1}{21}\sum_{h=0}^{20}\theta_h^2}$ of the true impulse response function prior to averaging across DGPs. See caption for Figure 6.2 for an explanation of the abbreviations in the legend.

across DGPs, we censor them above at 90% so that over-coverage is not rewarded. The picture that emerges is yet again consistent with our theoretical and practical messages: VAR and shrinkage confidence intervals can be quite a bit shorter, but this tends to come at the cost of (sometimes material) under-coverage, in particular at longer horizons. The VAR specifications with longer lag lengths yield correct coverage only at those horizons where the VAR confidence intervals are essentially as wide as those of LP.

Appendix E Probability of the VAR estimate falling outside the LP interval

In the theoretical framework of Section 3.3, the probability that the VAR estimate falls outside the LP confidence interval equals

$$P\left(\left|\hat{\theta}_h^{\text{VAR}}-\hat{\theta}_h^{\text{LP}}\right|>\tau_{h,\text{LP}}z_{1-a/2}\right)\approx P\left(\left|N\left(b_h(p),\tau_{h,\text{LP}}^2-\tau_{h,\text{VAR}}(p)^2\right)\right|>\tau_{h,\text{LP}}z_{1-a/2}\right)$$
$$=P\left(\left|N\left(\frac{b_h(p)}{\tau_{h,\text{VAR}}(p)},\frac{\tau_{h,\text{LP}}^2}{\tau_{h,\text{VAR}}^2(p)}-1\right)\right|>\frac{\tau_{h,\text{LP}}}{\tau_{h,\text{VAR}}(p)}z_{1-a/2}\right),$$

Figure E.1: Probability that the VAR point estimates are contained in the LP percentile-t bootstrap confidence intervals, averaged across all DGPs (stationary and non-stationary, monetary and fiscal), by impulse response horizon. The VAR and LP lag lengths are selected using the AIC.

where the approximation becomes exact asymptotically, due to (3.2) and the fact that the asymptotic covariance of the VAR and LP estimators equals the variance of the VAR estimator, as shown by Montiel Olea, Plagborg-Møller, Qian, and Wolf (2024). Since the right-hand side above is increasing in the bias/standard-deviation ratio of the VAR estimator, the bound (3.3) implies that the probability is no greater than

$$P\left(\left|N\left(\sqrt{T\times\mathcal{M}}\times\sqrt{\frac{\tau^2_{h,\mathrm{LP}}}{\tau^2_{h,\mathrm{VAR}}(p)}-1},\frac{\tau^2_{h,\mathrm{LP}}}{\tau^2_{h,\mathrm{VAR}}(p)}-1\right)\right|>\frac{\tau_{h,\mathrm{LP}}}{\tau_{h,\mathrm{VAR}}(p)}z_{1-a/2}\right)$$
$$=P\left(\left|N\left(\sqrt{T\times\mathcal{M}},1\right)\right|>\frac{z_{1-a/2}}{\sqrt{1-\tau^2_{h,\mathrm{VAR}}(p)/\tau^2_{h,\mathrm{LP}}}}\right).$$

When $1-a=90\%$ and $\tau_{h,\mathrm{VAR}}(p)/\tau_{h,\mathrm{LP}}=0.4$, then the above probability bound equals 21.6% when $\sqrt{T\times\mathcal{M}}=1$, and 58.1% when $\sqrt{T\times\mathcal{M}}=2$. Hence, there exist DGPs with a moderate amount of misspecification for which it is quite likely that the LP interval does not contain the VAR estimate.

However, in our empirically calibrated simulation study in Section 6.4, the clear majority of VAR point estimates do lie inside the LP confidence interval. Figure E.1 illustrates, plotting the share of VAR point estimates that are inside the LP interval by impulse response horizon h, averaged over all (stationary and non-stationary, monetary and fiscal) DGPs. The share is throughout in excess of 80 per cent, and particularly high at short horizons, consistent

with our theoretical discussion.

References

Barnichon, R., and C. Brownlees (2019): "Impulse Response Estimation by Smooth Local Projections," *The Review of Economics and Statistics*, 101(3), 522–530.

Blanchard, O., and R. Perotti (2002): "An Empirical Characterization of the Dynamic Effects of Changes in Government Spending and Taxes on Output," *Quarterly Journal of Economics*, 117(4), 1329–1368.

Brüggemann, R., C. Jentsch, and C. Trenkler (2016): "Inference in VARs with conditional heteroskedasticity of unknown form," *Journal of Econometrics*, 191(1), 69–85.

Christiano, L. J., M. Eichenbaum, and C. L. Evans (1999): "Monetary policy shocks: What have we learned and to what end?," in *Handbook of Macroeconomics*, ed. by J. Taylor, and M. Woodford, vol. 1, chap. 2, pp. 65–148. Elsevier.

Giannone, D., M. Lenza, and G. E. Primiceri (2015): "Prior selection for vector autoregressions," *Review of Economics and Statistics*, 97(2), 436–451.

Herbst, E. P., and B. K. Johannsen (2024): "Bias in local projections," *Journal of Econometrics*, 240(1), 105655.

Inoue, A., and L. Kilian (2020): "The uniform validity of impulse response inference in autoregressions," *Journal of Econometrics*, 215(2), 450–472.

Jentsch, C., and K. G. Lunsford (2019): "The Dynamic Effects of Personal and Corporate Income Tax Changes in the United States: Comment," *American Economic Review*, 109(7), 2655–78.

Kilian, L. (1998): "Small-sample Confidence Intervals for Impulse Response Functions," *Review of Economics and Statistics*, 80(2), 218–230.

Lazarus, E., D. J. Lewis, J. H. Stock, and M. W. Watson (2018): "HAR Inference: Recommendations for Practice," *Journal of Business & Economic Statistics*, 36(4), 541–559.

Li, D., M. Plagborg-Møller, and C. K. Wolf (2024): "Local projections vs. VARs: Lessons from thousands of DGPs," *Journal of Econometrics*, 244(2), 105722, Themed Issue: Macroeconometrics.

Montiel Olea, J. L., and M. Plagborg-Møller (2021): "Local Projection Inference Is Simpler and More Robust Than You Think," *Econometrica*, 89(4), 1789–1823.

Montiel Olea, J. L., M. Plagborg-Møller, E. Qian, and C. K. Wolf (2024): "Double Robustness of Local Projections and Some Unpleasant VARithmetic," Working Paper 32495, National Bureau of Economic Research.

Pope, A. L. (1990): "Biases of Estimators in Multivariate Non-Gaussian Autoregressions," *Journal of Time Series Analysis*, 11(3), 249–258.

Ramey, V. A. (2016): "Macroeconomic Shocks and Their Propagation," in *Handbook of Macroeconomics*, ed. by J. B. Taylor, and H. Uhlig, vol. 2, chap. 2, pp. 71–162. Elsevier.

Stock, J. H., and M. W. Watson (2016): "Dynamic factor models, factor-augmented vector autoregressions, and structural vector autoregressions in macroeconomics," in *Handbook of Macroeconomics*, vol. 2, chap. 8, pp. 415–525. Elsevier.